Precise measurement of HFS of positronium

A Ishida[1], G Akimoto[1], K Kato[1], T Suehara[1], T Namba[1], S Asai[1], T Kobayashi[1], H Saito[2], M Yoshida[3], K Tanaka[3], A Yamamoto[3], I Ogawa[4], S Kobayashi[4] and T Idehara[4]

[1] Department of Physics and ICEPP, the University of Tokyo, 7-3-1 Hongo, Bunkyo-ku, Tokyo, 113-0033, Japan

[2] Institute of Physics, the University of Tokyo, 3-8-1 Komaba, Meguro-ku, Tokyo, 153-8902, Japan

[3] High Energy Accelerator Research Organization (KEK), 1-1 Oho, Tsukuba, Ibaraki, 305-0801, Japan

[4] FIR Center, University of Fukui, 3-9-1 Bunkyo, Fukui, 910-8507, Japan

E-mail: ishida@icepp.s.u-tokyo.ac.jp

Abstract. The ground state hyperfine splitting in positronium, Δ_{HFS}, is sensitive to high order corrections of QED. A new calculation up to $O(\alpha^3)$ has revealed a $3.9\,\sigma$ discrepancy between the QED prediction and the experimental results. This discrepancy might either be due to systematic problems in the previous experiments or to contributions beyond the Standard Model. We propose an experiment to measure Δ_{HFS} employing new methods designed to remedy the systematic errors which may have affected the previous experiments. Our experiment will provide an independent check of the discrepancy. The measurement is in progress and a preliminary result of $\Delta_{\mathrm{HFS}} = 203.399 \pm 0.029\,\mathrm{GHz}\,(143\,\mathrm{ppm})$ has been obtained. A measurement with a precision of $O(1)$ ppm is expected within a few years.

1. Introduction

Positronium (Ps), a bound state of an electron and a positron, is a purely leptonic system which allows for very sensitive tests of QED. The precise measurement of the hyperfine splitting between orthopositronium (o-Ps, 1^3S_1) and parapositronium (p-Ps, 1^1S_0) (Ps-HFS) provides a good test of bound state QED. Ps-HFS is expected to be relatively large (for example compared to hydrogen HFS) due to a relatively large spin-spin interaction, and also due to the contribution from vacuum oscillation (o-Ps $\rightarrow \gamma^* \rightarrow$ o-Ps). The contribution from vacuum oscillation is sensitive to new physics beyond the Standard Model.

Figure 1 shows the measured and theoretical values of Ps-HFS. The combined value from the results of the previous 2 experiments is $\Delta_{\mathrm{HFS,exp}} = 203.388\,65(67)\,\mathrm{GHz}\,(3.3\,\mathrm{ppm})$ [1, 2]. Recent developments in nonrelativis-

tic QED (NRQED) have added $O(\alpha^3)$ corrections to the theoretical prediction which now stands at $\Delta_{\mathrm{HFS,th}} = 203.391\,69(41)\,\mathrm{GHz}$ $(2.0\,\mathrm{ppm})$ [3]. The discrepancy of $3.04(79)\,\mathrm{MHz}\,(15\,\mathrm{ppm},\,3.9\,\sigma)$ between $\Delta_{\mathrm{HFS,exp}}$ and $\Delta_{\mathrm{HFS,th}}$ might either be due to the common systematic uncertainties in the previous experiments or to new physics beyond the Standard Model.

There are two possible common systematic uncertainties in the previous experiments. One is the unthermalized o-Ps contribution which results in an underestimation of the material effect. This effect has already been shown to be significant [4]. The other is the uncertainty in the magnetic field uniformity which was cited as the most significant systematic error by previous experimenters.
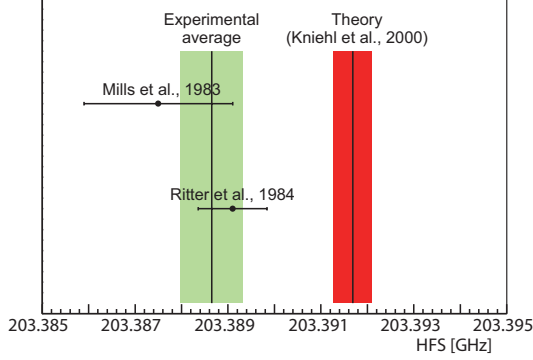
Figure 1. Measured and theoretical values of Ps-HFS.

Figure 2. Zeeman energy levels of Ps in its ground state.

2. Experimental setup

The energy levels of the ground state of Ps are shown as a function of static magnetic field in Figure 2. Due to technical difficulties in directly stimulating Δ_{HFS}, we make an indirect measurement by stimulating the transition Δ_{mix}. This is the same approach as previous experiments. The relationship between Δ_{HFS} and Δ_{mix} is given by the Breit-Rabi equation

$$\Delta_{\mathrm{mix}} = \frac{1}{2}\Delta_{\mathrm{HFS}}\left(\sqrt{1+x^2}-1\right), \quad (1)$$

in which $x = 2g'\mu_B H/h\Delta_{\mathrm{HFS}}$. $g' = g\left(1-\frac{5}{24}\alpha^2\right)$ is the g factor for a positron (electron) in Ps [5], μ_B is the Bohr magneton, H is the static magnetic field, and h is the Plank constant.

In a static magnetic field, the p-Ps state mixes with the $m_z = 0$ substate of o-Ps hence the latter state annihilates into 2 γ-rays with a lifetime of about 8 ns (with our experimental conditions). The $m_z = \pm 1$ substates of o-Ps annihilate into 3 γ-rays with a lifetime of about 140 ns. When a microwave field with a frequency of Δ_{mix} is applied, transitions between the $m_z = 0$ and $m_z = \pm 1$ substates of o-Ps are induced so that the 2 γ-ray annihilation rate increases. This increase is our experimental signal.

Following are the main improvements in our experiment which we expect will significantly reduce systematic errors present in previous experiments.
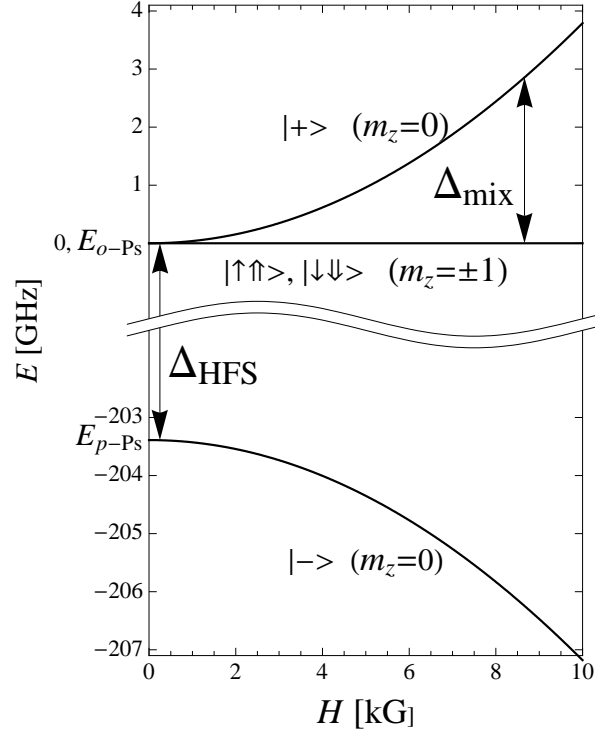
2.1. Large bore superconducting magnet (Figure 3)

A large bore superconducting magnet is used to produce the magnetic field which induces the Zeeman splitting ($\sim 0.866\,\mathrm{T}$). The bore diameter of the magnet is 800 mm, and its length is 2 m. The large bore diameter means that there is good uniformity in the magnetic field in the region where Ps is formed (70 ppm at 0.61 G without utilization of any compensation).

Furthermore, the magnet is operated in persistent current mode, making the stability of the magnetic field better than 1 ppm.

2.2. β-tagging system and timing information

The positron source is $19\,\mu\mathrm{Ci}$ (700 kBq) of ^{22}Na. A plastic scintillator 10 mm in diameter and 0.2 mm thick is used to tag positrons emitted from the ^{22}Na. The scintillation light

(a) The large bore superconducting magnet and the microwave waveguide. Microwaves are guided through the waveguide into the cavity.
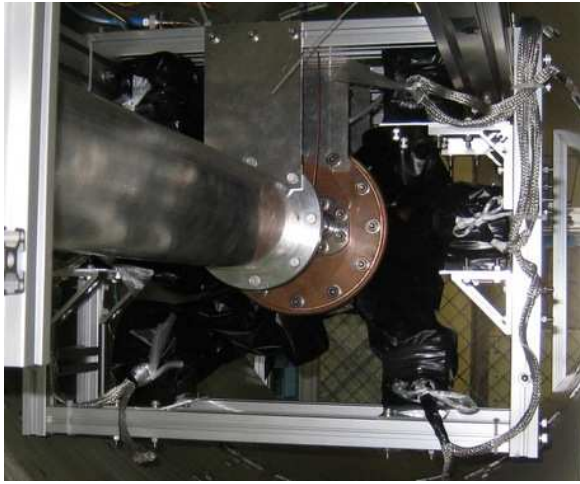
(b) Inside of the magnet. The β-tagging system, the γ-ray detectors and the microwave cavity are located at the center of the magnet.

Figure 3. Photographs of the experimental setup.

is detected by photomultipliers and provides a start signal which corresponds to the time of Ps formation.

The positron then enters the microwave cavity, forming Ps in the N_2 gas contained therein.

Ps decays into photons that are detected with $LaBr_3$ (Ce) scintillators. Accumulating measurements of the times of positron emission and γ-detection results in decay curves of Ps as shown in Figure 4. The timing information is used to improve the accuracy of the measurement of Δ_{HFS} as follows:

(i) Imposing a time cut means that we can select well thermalized Ps, reducing the unthermalized o-Ps contribution. It should also be possible to precisely measure the contributions of unthermalized o-Ps, and of material effects (we plan to make such measurements in future runs).

(ii) A time cut also allows us to avoid the prompt peak (contributions of simple annihilation and of fast p-Ps decay), which greatly increases the S/N of the measurement.

2.3. High performance γ-ray detectors

Six γ-ray detectors are located around the microwave cavity to detect the 511 keV annihilation γ-rays. $LaBr_3$ (Ce) scintillators, 1.5 inches in diameter and 2 inches long are used. $LaBr_3$ (Ce) scintillators have good energy resolution (4 % FWHM at 511 keV) and timing resolution (0.2 ns FWHM at 511 keV), and have a short decay constant (25.6 ns). The good energy resolution and the high counting rate of $LaBr_3$ results in very good overall performance for measuring 2γ decays. In particular the good energy resolution allows us to efficiently separate 2γ events from 3γ events, negating the need to use a back-to-back geometry to select 2γ events, thus greatly increasing the acceptance of our setup.

This γ-ray detector system greatly reduces the statistical error in the measurement.

2.4. RF system

Microwaves are produced by a local oscillator signal generator and amplified to 500 W with a GaN amplifier (R&K A2856BW200-5057-R).

The microwave cavity is made with oxgen-free copper; the inside of the cavity is a cylinder 128 mm in diameter and 100 mm long. The side wall of the cavity is only 2 mm thick in order to allow the γ-rays to efficiently escape. The cavity is operated in the TM_{110} mode. The resonant frequency is 2.8532 GHz and $Q_L = 14700 \pm 50$. The cavity is filled with 1.5 atm gas (90 % N_2 and 10 %
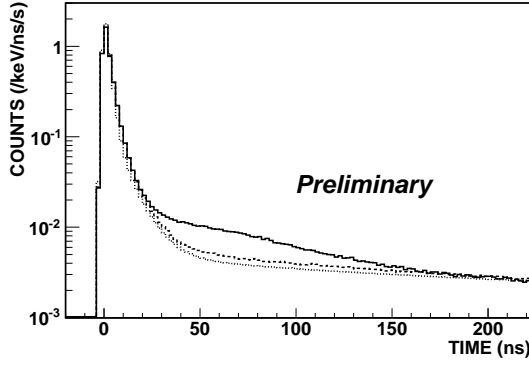
Figure 4. Decay curves of Ps at different magnetic field strengths. The solid line is 0.8659 T RF 450 W, the dashed line is 0.8614 T RF 450 W, and the dotted line is RF OFF. An energy window of 492–530 keV is applied.

iso-C_4H_{10}) with a gas-handling system. Iso-C_4H_{10} is used as the quenching gas to remove background 2 γ-ray annihilations.

3. Analysis and current status

The first run of the experiment is ongoing using the large bore magnet with no compensation (compensation magnets to reduce the uniformity to $O(1)$ ppm are planned but are not yet installed). The 2 γ-ray annihilation rate has been measured at various magnetic field strengths with a fixed rf frequency.

3.1. Data analysis

Figure 4 shows examples of measured timing spectra. The peak coming from prompt annihilation and p-Ps decay is followed by the decay curve of o-Ps and then the constant accidental spectrum. A timing window of 30–200 ns is applied to select o-Ps events. Figure 5 shows the 2γ transition spectrum, which is obtained as follows:

  (i) The accidental contribution is subtracted using the timing window $t =$ 700–900 ns.

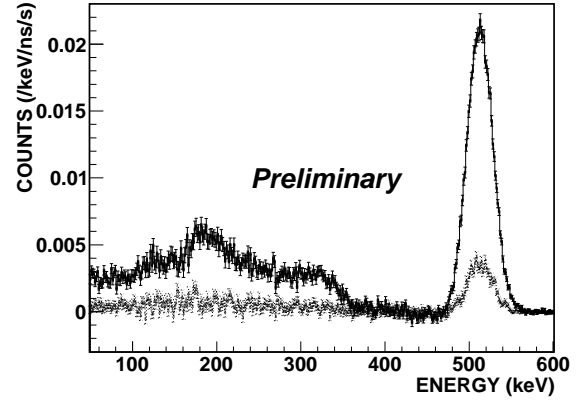 (ii) The ordinary o-Ps decay spectrum is also subtracted. This spectrum is

Figure 5. Energy spectra at different magnetic field strengths. The solid line is 0.8659 T RF 450 W and the dashed line is 0.8614 T RF 450 W. A timing window of 30–200 ns is applied, and the accidental spectra from 700–900 ns and RF OFF have been subtracted.
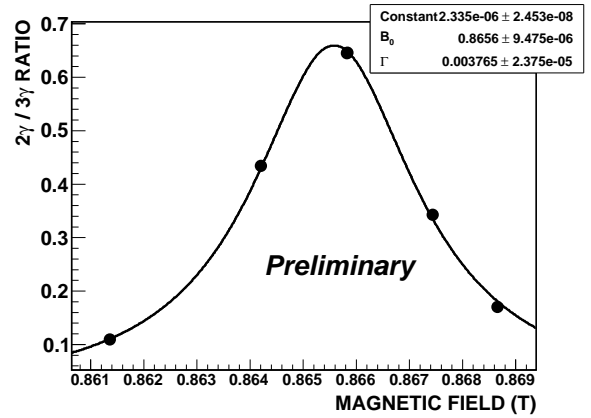

Figure 6. Resonance line at 1.5 atm. The data are fitted with the Breit-Wigner function (Equation (2)). Error bars are smaller than the marker size.

obtained by running without RF power, and is normalized to the 2γ transition spectrum in the region 380–460 keV.

The 2γ transition spectrum is measured at different magnetic field strengths. The resonance line obtained is shown in Figure 6.

Fitting the measured points with the Breit-Wigner function,

$$f(B) = \frac{C}{(B - B_0)^2 + \Gamma^2/4}, \qquad (2)$$

results in a constant of $C = 2.335(25) \times 10^{-6}$, a center value of the magnetic field of $B_0 = 0.865\,6151(99)\,\text{T}$ (11 ppm), and a width of $\Gamma = 3.765(24) \times 10^{-3}\,\text{T}$.

The main source of systematic error is the uniformity of the magnetic field (142 ppm in Δ_{HFS}). Other sources are considered to be negligible. The preliminary value of Δ_{HFS} calculated from equation (1) is

$$
\begin{aligned}
\Delta_{\text{HFS}} \quad = \quad & 203.399 \\
& \pm 0.005(\text{stat.}) \pm 0.029(\text{sys.}) \\
& \text{GHz} \,(143\,\text{ppm}), \qquad (3)
\end{aligned}
$$

which is consistent with both of the previous experimental values and with the theoretical value.

3.2. Future plan

The following improvements are planned for future measurements:

(i) Compensation magnets will be installed and $O(1)\,\text{ppm}$ magnetic field uniformity is expected to be achieved.

(ii) Measurements at various pressures of N_2 will be performed to estimate the material effect (the Stark effect). The accumulation of these measurements will result in an $O(1)$ ppm statistical error within a few years.

(iii) The timing information allows for a measurement of Ps thermalization as a function of time [4]. We can thus precisely measure the material effect including the thermalization effect.

4. Conclusion

A new experiment to measure the Ps-HFS which reduces possible common uncertainties in previous experiments has been constructed and the first run is ongoing. A preliminary value of $\Delta_{\text{HFS}} = 203.399 \pm 0.005(\text{stat.}) \pm 0.029(\text{sys.})\,\text{GHz}\,(143\,\text{ppm})$ has

been obtained, which is consistent with both of the previous experimental values and with the theoretical calculation. Development of compensation magnets is underway with a view to obtaining $O(1)\,\text{ppm}$ magnetic field homogeneity for future runs. A new result with an accuracy of $O(1)\,\text{ppm}$ will be obtained within a few years which will be an independent check of the discrepancy between the present experimental values and the QED prediction.

References
[1] Ritter M W, Egan P O, Hughes V W and Woodle K A 1984 *Phys. Rev.* B **30** 1331
[2] Mills A P Jr 1983 *Phys. Rev.* A **27** 262
[3] Kniehl B A and Penin A A 2000 *Phys. Rev. Lett.* **85** 5094
[4] Kataoka Y, Asai S and Kobayashi T 2009 *Phys. Lett.* B **671** 219
[5] Grotch H and Hegstorm R A 1971 *Phys. Rev.* A **4** 59